Drosophila *sosie* functions with β_H-Spectrin and actin organizers in cell migration, epithelial morphogenesis and cortical stability

Olivier Urwyler*, Fabiola Cortinas-Elizondo and Beat Suter‡

Institute of Cell Biology, University of Bern, Baltzerstrasse 4, 3012 Bern, Switzerland

*Present address: Vesalius Research Center, Flanders Institute of Biotechnology (VIB), University of Leuven (KUL), 3000 Leuven, Belgium

‡Author for correspondence (beat.suter@izb.unibe.ch)

Biology Open 1, 994–1005
doi: 10.1242/bio.20122154
Received 1st June 2012
Accepted 26th June 2012

Summary

Morphogenesis in multicellular organisms requires the careful coordination of cytoskeletal elements, dynamic regulation of cell adhesion and extensive cell migration. *sosie* (*sie*) is a novel gene required in various morphogenesis processes in Drosophila oogenesis. Lack of *sie* interferes with normal egg chamber packaging, maintenance of epithelial integrity and control of follicle cell migration, indicating that *sie* is involved in controlling epithelial integrity and cell migration. For these functions *sie* is required both in the germ line and in the soma. Consistent with this, Sosie localizes to plasma membranes in the germ line and in the somatic follicle cells and is predicted to present an EGF-like domain on the extracellular side. Two positively charged residues, C-terminal to the predicted transmembrane domain (on the cytoplasmic side), are required for normal plasma membrane localization of Sosie. Because *sie* also contributes to normal cortical localization of β_H-Spectrin, it appears that cortical β_H-Spectrin mediates some of the functions of *sosie*. *sie* also interacts with the genes coding for the actin organizers Filamin and Profilin and, in the absence of *sie* function, F-actin is less well organized and nurse cells frequently fuse.

Key words: Drosophila oogenesis, Spectrin, Morphogenesis, Cell migration, Cortical organization and stability, Epithelia

Introduction

During development, epithelial cells undergo dramatic morphogenetic rearrangements with concerted cell migrations and these events are essential for shaping epithelia and for forming organs. Drosophila oogenesis is an excellent model to study the genetic basis of epithelial morphogenesis and remodeling in an intact multicellular organism. In Drosophila, oogenesis unfolds in string-like subunits of the ovary, called ovarioles, which represent a sequence of different developmental stages. At the tip of an ovariole, in the germarium, stem cells for the germ line and the somatic follicle cells, respectively, produce the cells that assemble into egg chambers and ovarioles. One of the daughters of the germ line stem cell, the cystoblast, undergoes four rounds of mitotic divisions that are accompanied by incomplete cytokinesis. This results in a cyst of 16 germ line cells that remain interconnected to each other via specialized cytoplasmic bridges named ring canals. One of these cells differentiates into the oocyte, while the remaining 15 cells adopt a nurse cell fate. The nurse cells provide the oocyte with RNAs, proteins and organelles during the course of oogenesis. The 16 cell cysts are then surrounded by somatic follicle cells (FC) that originate from FC stem cells located in the middle of the germarium (Margolis and Spradling, 1995). The daughters of the FC stem cells first extend thin centripetal processes and then migrate around nascent cysts to envelop them as a monolayered epithelium, thereby separating adjacent cysts from each other (Dobens and Raftery, 2000).

At the posterior end of the germarium, single cysts are fully surrounded by their follicle cell epithelium and bud off as individual stage 1 egg chambers (Spradling, 1993). From stage 2 to 14, egg chambers grow to give rise to a mature egg. To accommodate the substantial growth of the germ line, follicle cells covering the surface of the cyst continue to grow and proliferate during the early stages of oogenesis, until their total number reaches around 650 (Margolis and Spradling, 1995). At stage 9, the follicle cell epithelium undergoes dramatic morphogenetic rearrangements. Most of the follicle cells undergo a collective posterior migration over the germ line and towards the oocyte, accompanied by a transition from a cuboidal to a columnar epithelium to fit over the oocyte surface (Montell, 2008). The few follicle cells that remain to cover the nurse cells adopt a squamous shape. Simultaneously, a group of 6–10 follicle cells at the anterior pole of the egg chamber delaminates from the epithelium and undergoes invasive migration through the nurse cells and towards the oocyte. This process is known as the border cell (BC) migration (Montell, 2008). Remodeling of the actin cytoskeleton is essential for cell shape change, migration and morphogenesis. Filamentous actin accumulates at the apical cortex of follicle cells (Baum and Perrimon, 2001) and defects in genes coding for actin-binding and actin-regulating proteins can

cause defects in the morphogenesis of the follicle cell epithelium and defects in BC migration.

The Spectrin-based membrane skeleton acts as a dynamic scaffold, one function of which is to anchor actin filaments at the cell cortex (reviewed by Thomas, 2001). Its primary building blocks consist of elongated tetramers of two α and two β Spectrin subunits. Each Spectrin tetramer has two actin binding domains, located at the N-termini of the two β subunits. Anchoring of such Spectrin filaments to the cell membrane occurs via binding to integral membrane proteins, either directly or via adaptor proteins such as Ankyrin or protein 4.1. The Spectrin cytoskeleton is polarized by the incorporation of different β subunits in different domains along the apicobasal axis. α-Spectrin associates with β-Spectrin in basolateral and with β_{Heavy} (β_H)-Spectrin in apical domains. While genetic studies have led to the rejection of a long-proposed central role for the Spectrin skeleton in establishing general apicobasal polarity, such studies have revealed essential functions of Spectrins for morphogenesis of epithelia (Thomas, 2001). In the Drosophila ovary, α-Spectrin is required in the follicle cell epithelium for maintenance of its monolayered organization (Lee et al., 1997) and β_H-Spectrin mutants cause abnormalities in follicle cell migration during mid-oogenesis and structural changes in follicle cells and the germ line (Zarnescu and Thomas, 1999).

Here we report the identification of *sosie*, a thus far uncharacterized gene that is involved in the formation of the follicle cell epithelium and in establishing the egg chamber structure early in Drosophila oogenesis. During the BC migration phase it is involved in coordinating this process with follicle cell migration. *sosie* interacts with β_H-Spectrin, is required for normal localization of β_H-Spectrin and is involved in the maintenance of structures of the Spectrin and actin cytoskeletons during oogenesis. Interestingly, *sosie* encodes a predicted small transmembrane protein with an EGF-like domain and its product seems to localize to apical plasma membranes. Two positively charged residues adjacent to this transmembrane domain in the short C-terminal (cytoplasmic) tail are essential for normal plasma membrane localization of Sosie::Venus.

Results

Identification of *sosie*, a novel gene involved in egg chamber formation

Mutations in the previously uncharacterized gene *CG13636* in the cytological region 96A/B dominantly suppress the double abdomen phenotypes caused by $Bic\text{-}D^{IIIE48}$ (supplementary material Fig. S1). Because *Bic-D* has well characterized functions in oogenesis (Mohler and Wieschaus, 1986; Suter and Steward, 1991; Ran et al., 1994; Swan and Suter, 1996), we set out to analyze oogenesis in *CG13636* mutants. The Exelixis PiggyBac (Thibault et al., 2004) transposon insertion lines c03947 and f00514 (sie^1 and sie^2, respectively) (Fig. 1A) show defects in egg chamber formation when homozygous or hemizygous. A transgenic copy of *CG13636* extending from 1.5 kb upstream into the next downstream gene was able to revert efficiently the defects observed in sie^2 mutants, indicating that *CG13636* is indeed involved in egg chamber formation during Drosophila oogenesis (supplementary material Fig. S2). In these mutants we found compound egg chambers with more than the normal 16 germ cells and more than one oocyte (Fig. 1A–C). Because two oocytes in one egg chamber very much look alike, the *CG13636* gene was named *sosie* (*sie*), which is French for a "look-alike". Furthermore, rarely we also observe fewer germ cells in an egg chamber (not shown), pointing to defective encapsulation of germ cell clusters by the somatic follicle cells (Goode et al., 1992; Sokol and Cooley, 2003). sie^1 and sie^2 oocytes have the normal amount of four ring canals, indicating that the germ line went through the normal number of four incomplete divisions (Fig. 1B, inset) and that the compound egg chambers are not generated by an additional division of the germ cell cluster. This interpretation is also consistent with the observation that in sie^1 and sie^2 compound egg chambers the two oocytes are separated from each other and that later developmental stages contain nurse cell clusters of strongly differing ploidy and age (Fig. 1C). Therefore, the compound egg chambers in the *sie* mutants are derived from multiple cystocyte clusters and this phenotype reflects a defective packaging of individual germ line cysts into discrete egg chambers by the somatic follicle cells. Most *sie* egg chambers with an abnormal number of germ line cells degenerate at later stages of oogenesis (not shown).

The *sosie* alleles

Egg chamber defects in the *sosie* PiggyBac insertion mutants sie^1 and sie^2 occurred with varying penetrance, ranging from few percentages up to around 65% of egg chambers, with no clear dependence on temperature, food conditions or age of the flies. *sosie* females and males remain fertile (supplementary material Fig. S2). We therefore tested whether sie^2 still produces a gene product. Indeed, RT-PCR analyses using the primers shown in Fig. 1A revealed the presence of both upstream and downstream exons of *sie*, but no or only spurious amounts of PCR products are detected with primers spanning the transposon insertion site (Fig. 1D). In an attempt to isolate a *sie* null allele, we next created deletions of the *sosie* locus by imprecise transposon excision. Because re-mobilization of PiggyBac transposons almost always occurs by precise excision (Thibault et al., 2004), we used a Minos transposon inserted near the 3′-splice site of the last *sosie* intron ($CG13636^{MB03846}$, termed sie^3) (Fig. 1A) (Metaxakis et al., 2005). Out of more than 500 remobilization events, 2 imprecise excisions (sie^4 and sie^5) were isolated and the extension of the deficiencies determined by sequencing. They delete the last 3 and 2 *sosie* exons, respectively (Fig. 1A). sie^4 deletes most of the open reading frame, but also part of the predicted neighbor gene *CG33658*. On the other hand, the first *sosie* exon is still expressed and polyadenylated (Fig. 1D). Both deletion mutants showed the same phenotypes as sie^1 and sie^2 with similar, but variable, penetrance and they are homo- and hemizygous viable and remain fertile.

sosie's role in germarial follicle cell migration and epithelial integrity

Egg chamber packaging problems can arise if the follicle cells in the germarium fail to properly differentiate. In mutants of the Delta/Notch signaling pathway no stalks are formed between individual egg chambers due to the failure of follicle cells to differentiate at the poles of the egg chambers (Ruohola et al., 1991; Goode et al., 1996; López-Schier and St Johnston, 2001). In such cases, the double-layered epithelium separating adjacent cysts degenerates during mid-oogenesis, leading to fused egg chambers mainly after stage 7 (Torres et al., 2003; López-Schier and St Johnston, 2001). In contrast, *sosie* mutant ovaries frequently contain younger egg chambers with more than the

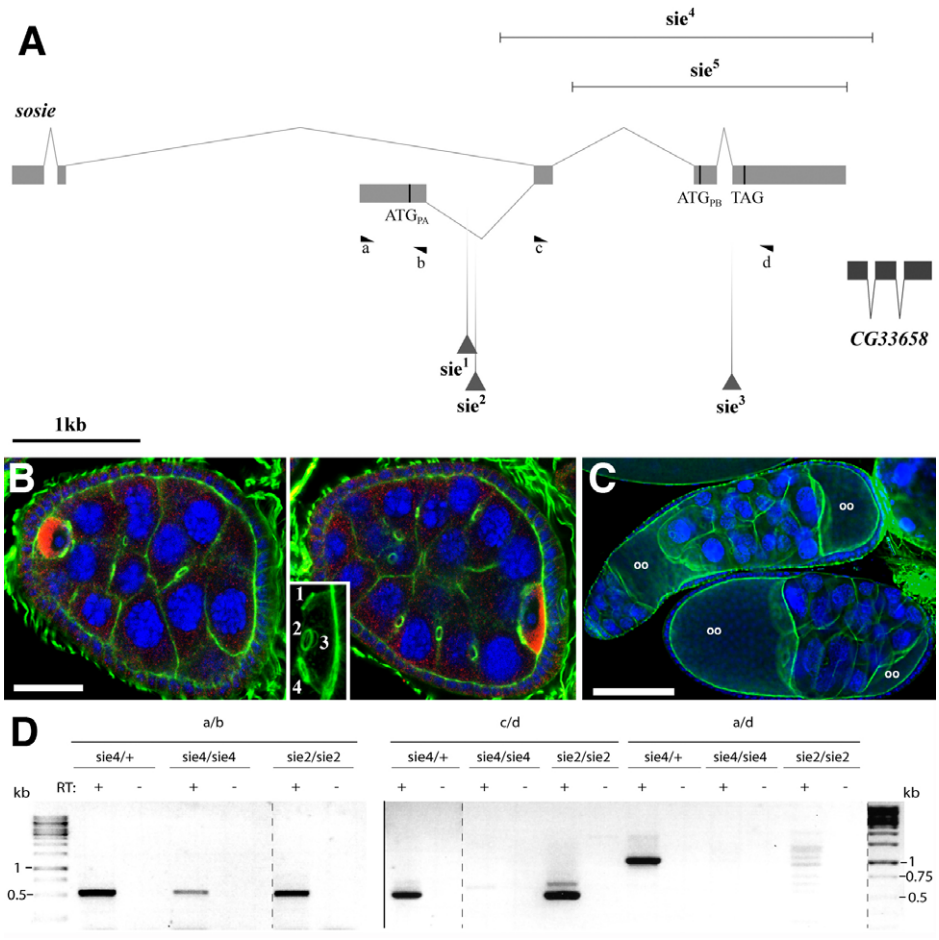

Fig. 1. *sosie* genetics and compound egg chamber phenotype. (**A**) The *sosie* locus and its mutants (adapted from Flybase: http://flybase.org). Exons are shown as solid boxes, connecting lines represent introns. Start codons (ATG) of two different predicted *sosie* open reading frames (ORF) RA and RB, respectively (encoding PA and PB, respectively) are indicated as vertical bars. They are in the same frame ending with TAG. RA is the major transcript in adult females, but there is also evidence for a third, minor transcript, RC, that initiates 1.6 kb downstream of RB, encodes the small PB ORF and is mainly expressed in pupae and adult males. Transposon insertions are shown as triangles. sie^1 and sie^2 are the Exelixis PiggyBac insertions c03947 and f00514, respectively. sie^3 is the Minos transposon insertion MB03846, which was used to create deletions sie^4 and sie^5 by imprecise excision (indicated as horizontal lines). The predicted *sosie*/*CG13636-RB* mRNA splice variant (top) with the ATG_{PB} start codon in its fourth exon could not be detected by RT-PCR from ovarian extracts, and only one expressed sequence tag (EST) was listed on http://flybase.org for *CG13636-RB* at the time when 12 ESTs were found for *CG13636-RA*. The positions and orientations of the primers used for the RT-PCR shown in D are also indicated (a–d). The neighbor gene *CG3368* is encoded on the opposite strand. (**B**) Compound egg chamber in a sie^1/Df(3R)Exel6200 ovary. Two focal planes of the same egg chamber are shown and the inset is a magnification of the oocyte at the posterior of the compound egg chamber, revealing the presence of four ring canals. Blue: DNA. Green: filamentous actin. Red: Egalitarian (oocyte marker). The nurse cells are easily recognizable by their big polyploid nuclei (blue). Note that the egg chamber contains more than 16 germ line cells and two oocytes. Scale bar represents 20 µm. Posterior is to the right. (**C**) Compound egg chambers at later developmental stages in a sie^2/sie^2 ovary. The upper one contains even more than twice the normal complement of germ line cells and appears as a long tube of fused germ line cysts that are not separated by somatic follicle cells. Oocytes are labeled (oo). Blue: DNA. Green: F-actin. Scale bar represents 100 µm. (**D**) Expression of polyadenylated *sie* mRNA in heterozygous or homozygous *sie* mutant ovaries. Reverse transcription (RT) reactions were primed with oligo-dT. Lanes labeled with "−" are controls where the reverse transcriptase was omitted from the RT. a, b, c and d indicates the primers that were used for the individual PCRs (primer positions are shown in A). Products amplified with primer pair a/b were loaded on a separate agarose gel as indicated by the vertical separator line. Rearrangements of lanes within a gel are indicated by dashed vertical lines. The DNA molecular weight standard is shown on both sides.

normal complement of 16 germ line cells, suggesting that the packaging defect is caused by an earlier developmental problem (Fig. 2A). Furthermore, as opposed to defective Delta/Notch signaling, in *sie* mutants the FasciclinIII (FasIII) marker for undifferentiated follicle cells becomes properly restricted to polar cells in morphologically normal and the compound egg chambers, confirming that follicle cells do indeed differentiate (Fig. 2B).

To visualize the encapsulation defects as they arise, we studied the morphology of the germarial regions 2–3. Indeed, defects can already be found at the first stages of egg chamber formation in *sie* mutants, where encapsulation is frequently not completed, leaving adjacent germ line clusters connected to one another with no follicle cell layers between them (compare Fig. 2C with Fig. 2D). These findings suggest that *sosie* facilitates migration of follicle cells around nascent cysts as they move through germarial region 2, allowing the formation of an intact epithelium. Consistent with this view, we observe egg chambers with discontinuous follicle cell epithelia in all subsequent phases of oogenesis (Fig. 2E–G).

To find out whether *sie* is required in the germ line for egg chamber packaging and inclusion of 16 germ cells into a follicle, we performed RNAi knock down experiments using two different RNAi lines no. 1218 and no. 1219 (Dietzl et al., 2007).

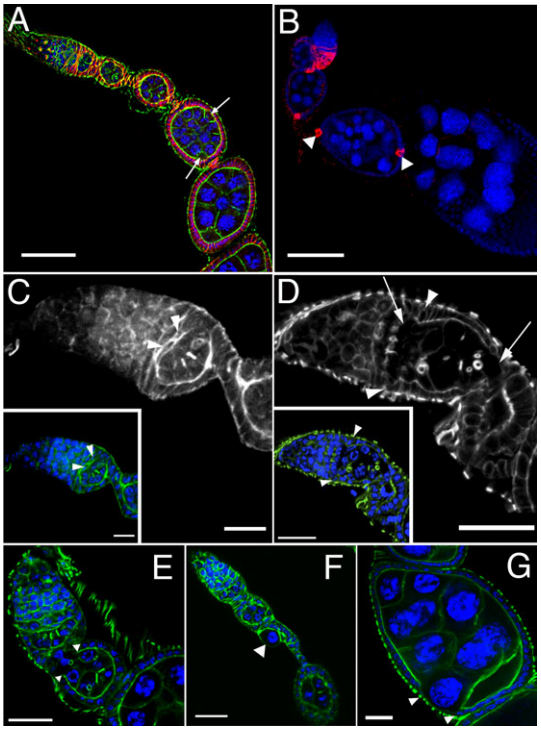

Fig. 2. *sosie* functions in encapsulating the germ line cysts in the germarium. DNA is shown in blue and F-actin in green in all colored panels. (**A**) Compound egg chamber containing 2 germ line cysts at an early developmental stage in a sie^4/sie^4 ovariole. Its oocytes are indicated by arrows. The compound egg chamber is flanked by a normal stage 3 egg chamber anteriorly, and by a normal stage 6 egg chamber posteriorly, indicating that it is a stage 4–5 egg chamber. Adducin-related protein/Hts staining is shown in red. (**B**) FasIII immunostaining (red) of a sie^1/Df(3R)Exel6200 ovariole. Arrowheads indicate proper restriction of FasIII signal to polar follicle cells after developmental stage 3 in a compound egg chamber. (**C**) F-actin staining in a wild-type germarium reveals follicle cells that extend F-actin-rich centripetal processes and migrate around the anterior border of a germ line cyst to encapsulate it (arrowheads). (**D**) sie^5/Df(3R)Exel6200 germarium. As revealed by F-actin staining, follicle cells fail to extend processes and to migrate around germ line cells (arrowheads), leading to an open continuum of germ line cells from germarial region 2 to 3 (arrows). (**E**) Open follicle cell epithelium at the anterior end of a budding sie^4/sie^4 egg chamber. Arrowheads indicate the borders of the epithelium. (**F**) Occasionally, single germ line cells that were not packaged into egg chambers can be observed. The arrowhead indicates such a polyploid pseudo-nurse cell in a sie^4/sie^4 ovariole. (**G**) A nurse cell appearing at the surface of a stage 7 sie^4/sie^4 egg chamber due to a gap in the follicle cell epithelium (arrowheads indicate its border). Anterior is top left and scale bars represent 50 µm in A,B, 10 µm in C, and 20 µm in D–G.

Considering that this type of knock down generally does not work in later stages in the female germ line (Rørth, 1998; Ni et al., 2011), we found evidence for a germ line requirement for *sie*. With the RNAi line no. 1218 5% (6/132) of the egg chambers showed abnormal germ cell numbers when using the germ line driver *matTubGAL4* on the second chromosome (supplementary material Table S1). On the other hand, we did not observe any packaging problems when expressing UAS-GFP with this driver as a control (0 egg chambers with abnormal germ cell numbers/90). From this it seems that *sie* is required in the germ line for packaging the normal number of germ cells into egg chambers. Phenotype and difference to control were, however, less pronounced in experiments with the second RNAi line, no. 1219 (supplementary material Table S1). The GAL4 driver *P{GawB}109-30* drives *UAS::GFP* expression in the follicle cells in the germarium and the early egg chamber stages until stage 3. When using this driver to knock down *sie* RNA expression, we observed neither packaging defects nor irregular numbers of germ cells (data not shown). While we cannot exclude that the follicle cell knock down is inefficient, these results may also mean that it is the germ line expression of Sie that produces a signal for the follicle cells.

Sosie localizes to plasma membranes and contains an EGF-like domain

In silico analysis of the 186 amino acids (aa) long protein encoded by the *sosie*-RA transcript (Fig. 1A) predicted a N-terminal signal peptide for targeting of the protein to the endoplasmic reticulum (ER) and a 22–23 aa long transmembrane domain in proximity of the C-terminus, which would span a lipid bilayer membrane once (Fig. 3A). In addition, between the predicted signal peptide and transmembrane domain there is a region of about 50 aa with sequence similarity to the epidermal growth factor (EGF) motif. The sequence identity between the Sosie EGF domain and the human transforming growth factor α (TGF-α) is 24.5%. For comparison, the Drosophila germ line TGF-α homologue Gurken and human TGF-α share 22.6% identity in their EGF domain. Most importantly, the cysteines that shape the structure of the EGF domain are also present (Fig. 3A) (Garrett et al., 2002). In the 4th and 3rd position before the C-terminus (−4 and −3), Sosie contains two basic amino acid residues, arginine and lysine (…RKHF-COOH). Di-lysine or di-arginine residues in these locations of a single-pass transmembrane (TM) protein can act as ER retention signals by binding the complex of cytosolic coat proteins, COPI, and this retrieves the protein from the Golgi to the ER (Teasdale and Jackson, 1996). In Drosophila Jagunal the di-basic sequence motif …RKXX at the C-term seems to serve the same function (Lee and Cooley, 2007). On the other hand, according to the "positive-inside rule" such basic charges seem to drive membrane protein topogenesis because the cytoplasmic side adjacent to the TM usually shows positively charged residues (Bogdanov et al., 2009). Furthermore, a diphenylalanine (FF) motif in positions −1 and −2 provides export from the ER for a vertebrate protein (Kappeler et al., 1997). The C-terminal Sosie …RKHF motif could therefore ensure its proper membrane insertion or it could serve as ER retention or ER export signal.

To analyze the subcellular localization of Sosie during oogenesis we produced a transgenic strain expressing a Sosie::Venus fusion protein under the control of the yeast upstream activating sequence UAS (Brand and Perrimon, 1993; Nagai et al., 2002). Venus was inserted just N-terminal to the transmembrane domain (Fig. 3A), to neither interfere with the signal peptide at the N-terminus nor with the function of the C-terminal sequence. Expressing the fusion protein under the control of either of the two germ line specific drivers *nanosGAL4* and *matTubGAL4*, the Sosie::Venus signal strongly accumulated primarily at the plasma membrane of the germ cells, including the ring canals (Fig. 3B–D; data not shown). Sosie::Venus signal was therefore not observed enriched in the ER (compare with Fig. 3E). This plasma membrane localization was not caused by the over expression of Sosie::Venus (which may overload the ER retention mechanism) because Sosie::Venus expressed from its own promoter produced a weak signal that is recognizably enriched on the germ line plasma membrane and on apical plasma

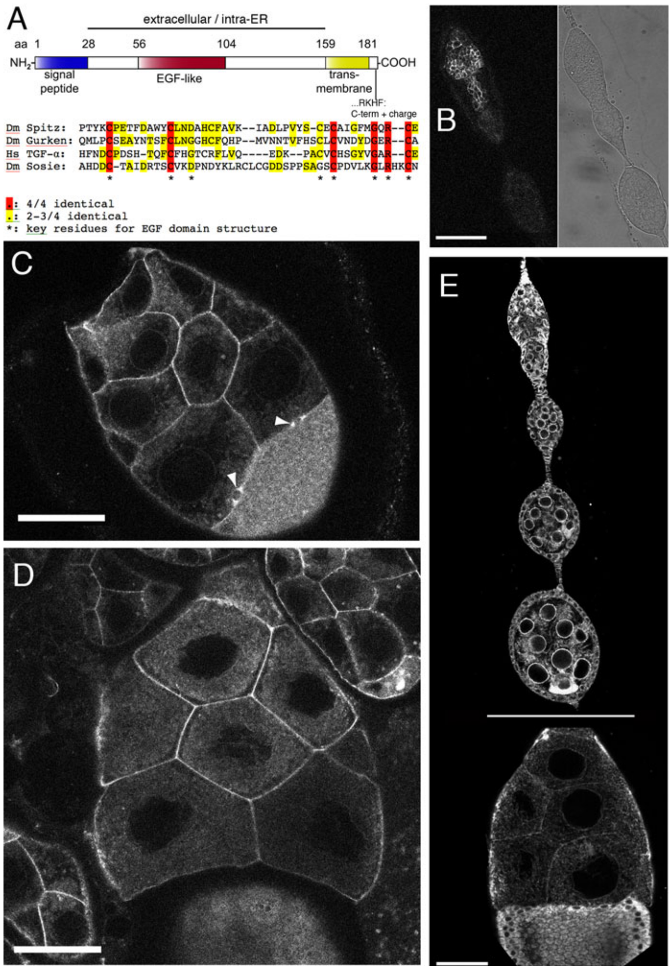

Fig. 3. Sosie protein structure and localization. (**A**) Schematic representation of the Drosophila melanogaster (Dm) Sosie protein (Fig. 1A, isoform PA). Computationally predicted domains are indicated. aa: amino acid. NH_2: N-terminus. COOH: C-terminus. EGF: epidermal growth factor. ER: endoplasmic reticulum. Hs: Homo sapiens. Another program predicts the signal peptide from aa12–33 and the transmembrane domain from aa159–180 (http://phobius.sbc.su.se). (**B–D**) Distribution of Sosie::Venus in germ line cells (the UAS construct was driven by *nanosGAL4*). Scale bars represent 50 µm. (B) Germarium. Left panel, Sosie::Venus fluorescence, accumulating at cell membranes. Right panel, transmitted light image. (C) Stage 8 egg chamber. Note the strong Sosie::Venus signal on nurse cell membranes and on two ring canals between nurse cells and the oocyte (arrowheads). The uniformly distributed signal in the oocyte (bottom right) is likely to stem from yolk autofluorescence. (D) Stage 10 egg chamber. Sosie::Venus signal accumulates much stronger on plasma membranes than eYFP-ER (see E). (**E**) Appearance of the ER in the germ line and somatic cells of the ovary, visualized with an ER-targeted eYFP. The horizontal line indicates that the stage 10 egg chamber (bottom) was recorded in a different image. Note the prominent accumulation of signal around the nurse cell nuclei and at the oocyte posterior during early oogenesis. Scale bar represents 50 µm.

membranes of follicle cells (supplementary material Fig. S3). Notably the transgene used for these studies rescued the *sie* defects with a very similar efficiency as the untagged genomic transgene, indicating that the insertion of Venus does not affect *sie* function. In addition, in salivary glands Sie::Ven driven by a somatic GAL4 driver primarily accumulates at the apical plasma membrane (supplementary material Fig. S3). The presence of Sosie at the plasma membrane was also confirmed in a recent proteomics report (Khanna et al., 2010). Therefore, a significant proportion of the Sosie protein seems to expose its EGF-like domain to the extracellular space.

To test the function of the dibasic element close to the C-term we expressed from a transgene a variant Sosie::Venus, in which the C-terminal …RKHF sequence motif was replaced by …LNHF. This mutant showed an ER-like signal distribution (Fig. 4A–C), suggesting that the RK dipeptide serves a function in Sosie localization to the plasma membrane. We also observe a similar role for the RK dipeptide in the somatic follicle cells (Fig. 4D,D′).

Sosie cooperates with β_H-spectrin to coordinate epithelial cell migration

Until stage 8 the follicle cells cover the germ line homogenously as a cuboidal epithelium. Subsequently, most of the follicle cells migrate towards the posterior to form a columnar epithelium over the oocyte, leaving back a thin layer of squamous follicle cells covering the nurse cells. This migration event occurs in synchrony with the invasive migration of a small group of 6–10 anterior follicle cells, the border cells (BC), which make their way through the nurse cell cluster and towards the oocyte (Fig. 5A) (Montell et al., 1992). During normal oogenesis the two migration events are coordinated and occur in synchrony, but most of the time the *sie* mutations cause the border cells to

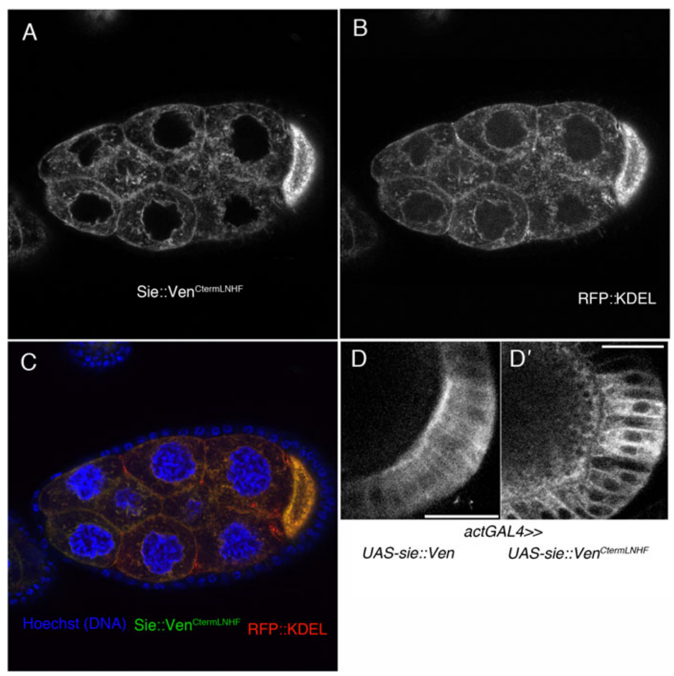

Fig. 4. C-terminal RK residues are required for Sosie plasma membrane localization. (**A–C**) Tangential section through a stage 9 egg chamber expressing Sosie::Venus with an altered C-terminal sequence and the ER marker KDEL::RFP both from an UAS promoter. Expression was driven by the germ line specific *matTubGAL4* driver. (A) Expression of Sosie::Venus with an altered C-terminal sequence (…LNHF instead of …RKHF) fails to produce a preferential plasma membrane signal. Instead, the signal resembles an ER staining. (B) Expression of the ER marker RFP:: KDEL. (C) Overlay of A and B showing also Hoechst staining for DNA (blue). Large nuclei are nurse cell nuclei, small ones are follicle cell nuclei. (**D**) Driven with the general driver *actGAL4*, wild type Sosie::Venus produces a signal that is enriched at the apical plasma membrane in follicle cells (D), while the C-term mutant Sosie::Venus^{CtermLNHF} produces a cytoplasmic or ER signal (**D′**). Scale bars represent 20 µm.

Biology Open

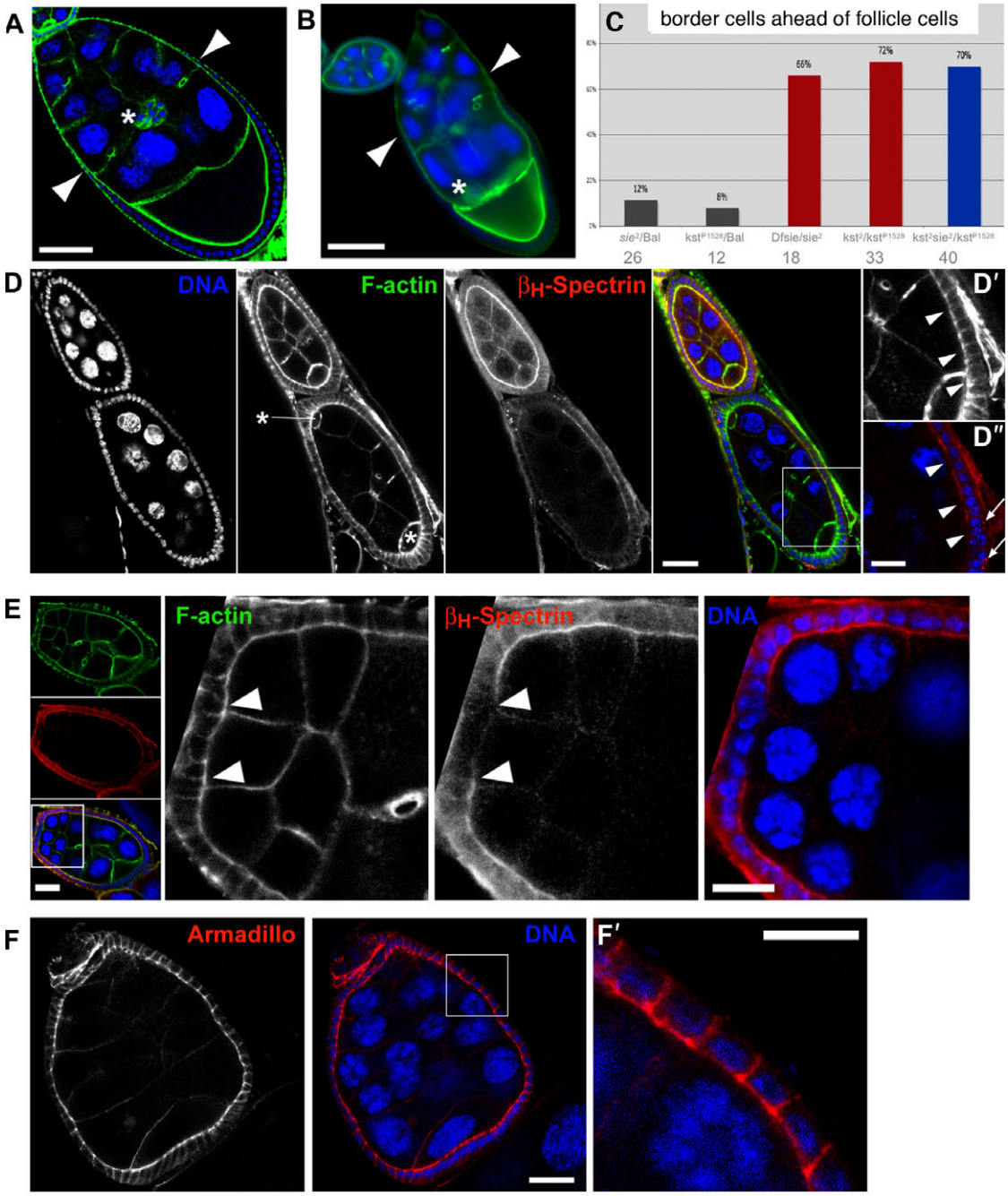

Fig. 5. Sie–kst/β_H-Spectrin interaction, BC/FC migration and maintenance of epithelial structures. (**A**,**B**) DNA is in blue and filamentous F-actin in green. Scale bars represent 50 µm. (A) Wild type stage 9 egg chamber with coordinated migration of BC (asterisk) and outer FC (arrowheads mark most anterior ones). (B) Stage 9 *sie*^{5}/Df(3R)Exel6200 egg chamber with BC (asterisk) that have already reached the oocyte while the most anterior outer FC (arrowheads) have not even completed half of their migration. (**C**) Quantification of mis-coordination between outer FC and BC migration in heterozygous, hemizygous and compound heterozygous *sosie* and *karst* mutants. See text for details. Bal stands for balancer chromosome, which is wild type for *sie* and *kst*. *Dfsie* is a small deficiency that removes *sie*. Numbers below the genotypes indicate the number of stage 8 to 9 egg chambers counted for each genotype. Having only one functional copy of *sie* in a *kst* background did not further enhance the frequency of this phenotype. (**D**) Disruption of apical β_H-Spectrin localization in follicle cells of a *sie*^{4}/*sie*^{4} compound egg chamber. Asterisks indicate the position of the two oocytes. **D′**,**D″** show a magnified view of the area boxed in the merge panel. Arrowheads point to the apical sides of follicle cells that have lost β_H-Spectrin signal (D″), while the appearance of F-actin (D′) seems normal. Arrows in D″ point to cytoplasmic puncta of β_H-Spectrin signal. Scale bars represent 20 µm in the main panels and 10 µm in D′,D″. (**E**) Anterior follicle cells of a *sie*^{2}/*sie*^{2} compound egg chamber have lost apical β_H-Spectrin signal. Left panels show an overview of the egg chamber. Note the difference in size and ploidy of the nurse cells that originated from two different cystoblasts. The boxed area denotes the region that is magnified in the panels on the right. In these, arrowheads point to the border between follicle cells that show normal apical accumulation of β_H-Spectrin signal and those in which apical β_H-Spectrin signal becomes virtually undetectable. Scale bars represent 20 µm in the overview panels and 10 µm in the panels showing a magnified view. (**F**) Adherens junctions appear normal and are precisely located in an apico-lateral position in a *sie*^{2}/*sie*^{2} compound egg chamber as assayed by immunostaining for Armadillo/β-catenin. **F′** shows a magnification of the area boxed in the middle panel. Scale bars represent 20 µm in F and 10 µm in F′, respectively.

migrate far ahead of the outer follicle cells (Fig. 5B). However, in rare cases we have also found them delayed (not shown).

To find out whether coordination of BC and FC migration requires *sie* in the germ line or in the soma or both, we knocked down *sie* using the RNAi lines described. In the RNAi line controls without a driver we observed that in 13% (no. 1218; $n=8$) and 6% (no. 1219; $n=17$) of the stage 9 egg chambers the BCs migrated ahead of the FCs. Similarly, in stage 9 egg chambers where the UAS-GFP control is driven with the *matTubGAL4* driver only 10% of the BC migrated ahead of the FC ($n=21$). In contrast, driving the *sie* RNAi lines with the germ line driver caused the BC to migrate ahead of the FC in 47% (no. 1218; $n=19$) and 65% (no. 1219; $n=17$) of stage 9 egg chambers (supplementary material Table S1). It is surprising that RNAi knock down in the germ line was able to reveal such a late germ line phenotype. However, it is also possible that RNAi depletion early in germ line differentiation caused another defect that is responsible for this later phenotype. To find out whether *sie* is also required in the somatic FC for coordination of BC and FC migration, we used the RNAi lines in combination with the follicle cell driver $GAL4^{109-79}$ to knock down *sie*. This construct drives expression from UAS sequences weakly in stage 7 and more strongly after this. When this driver was used to express the GFP control in the target cells, BC migration ahead of FC was only seen in 9% of the stage 9 egg chambers (2/22). When used to drive *sie* RNAi, BC migrating ahead of FC were found in 48% of stage 9 egg chambers (16/33 with no. 1218) and in 66% (19/29 with no. 1219), indicating clearly a somatic requirement for *sie* for the coordination of this ovarian cell migration (supplementary material Table S1).

The β_H-Spectrin gene *karst* is also required for coordination of BC and FC migration and loss of its activity also causes the BC to migrate ahead of the FC (Zarnescu and Thomas, 1999). Indeed, an initial analysis pointed to a genetic interaction between the two genes because double heterozygous combinations of *sosie* and *kst* alleles ($Dfsie$ +/+ kst^2) showed second site non-complementation for the phenotype in which BC migrate ahead of FC. In 65% ($n=77$) of the sampled double heterozygous egg chambers the border cells migrated ahead of the FC and penetrance and expressivity were stronger than a simple additive effect of the two individual heterozygous mutations (20% ($n=49$) and 9% ($n=35$); data not shown). To compare the function of *sosie* and *karst* in epithelial morphogenesis, we analyzed coordination of BC and FC migration in heterozygous and homozygous *sosie* and *karst* mutant females. For a semi-quantitative analysis of the coordination defect, we chose only samples where the follicle cells had moved between 20 and 110 µm. This ensured that we focused on the correct migration stage. Based on our observations with wild type egg chambers, we then used 10 µm difference in migration distance between FC and BC as the limit for normal range of movement coordination. BC migrating more than 10 µm ahead of the follicle cells were classified as "ahead". While heterozygous single mutations in either gene showed BC migrating ahead of FC in only 8–12% of the egg chambers (Fig. 5C), females with both copies of *sosie* inactivated showed 66%, while females mutant for both copies of *karst* showed BC migrating ahead of FC in 72% of the egg chambers. Interestingly, in flies that were mutant for *karst* ($kst^{2/P1528}$) the inactivation of one copy of *sosie* did not further increase the penetrance of this coordination defect. Like the similar phenotypes, this is consistent with the two genes acting in the same pathway.

β_H-Spectrin is expressed both in the germ line and in the somatic tissue of the Drosophila ovary. In the follicle cells, it localizes to apical membranes, where it forms heterotetramers with α-Spectrin (Zarnescu and Thomas, 1999). To determine whether *sie* is involved in polarized localization of β_H-Spectrin in follicle cells, we stained *sie* mutant ovaries with an antibody against β_H-Spectrin (Thomas and Kiehart, 1994). β_H-Spectrin signal accumulated at the apical membrane of follicle cells in morphologically normal sie^- egg chambers (Fig. 5D, upper egg chamber). In mutant egg chambers that display epithelial defects, we observed specific loss of apical β_H-Spectrin in follicle cells (Fig. 5D,D″, older egg chamber) and general loss of β_H-Spectrin signal (Fig. 5E), while the strong signal of the apical F-actin was still present and therefore less affected (Fig. 5D,D′, Fig. 5E). β_H-Spectrin localization is only affected in some sie^- follicle cells, suggesting that sie^+ may not be the sole factor that targets β_H-Spectrin to apical membranes. Interestingly, we sometimes observed punctae of strong β_H-Spectrin signal in the cytoplasm of follicle cells lacking apically localized β_H-Spectrin, indicating that non-localized β_H-Spectrin may accumulate at specific sites in the cytoplasm (Fig. 5D,D″).

General apicobasal polarity of follicle cells is normal in *kst* mutants (Zarnescu and Thomas, 1999). To determine whether *sie* is essential for establishment and/or maintenance of apicobasal polarity in the follicle cell epithelium, we analyzed the localization of adherens junctions in follicle cells. As in the wild type, in *sie* mutant ovaries Armadillo/β-catenin accumulates normally in the apical part of follicle cells, even in compound egg chambers (Fig. 5F) (Peifer et al., 1993), indicating that (like β_H-Spectrin) *sie* is not essential for establishing and maintaining general apicobasal polarity of follicle cells. These findings also suggest that loss of β_H-Spectrin from apical cell membranes in defective egg chambers is a specific consequence of *sie* disruption and not a secondary effect due to loss of general apicobasal polarity. We also analyzed the distribution of *D*E-Cadherin and Crumbs in the follicle cells. As long as the mutant follicle cells were still integrated in the epithelium, we were not able to observe changes in the distribution of *D*E-Cadherin or Crumbs (data not shown), indicating that *sie* is not essential for their normal distribution.

Older egg chambers of *sie* mutants also show changes in the cuboidal follicle cell layer, where the epithelial structure appears distorted. We confirmed that this is due to reduced *sie* activity by knocking down *sie* with RNAi in the follicle cells using the follicle cell driver *P{GawB}109–79* and the two *sie* RNAi constructs. With this approach we observed a clear increase in distorted follicle cell epithelia during late stages of oogenesis. In the combined RNAi analysis 25% (22/89) of the egg chambers analyzed showed irregular or distorted follicle cell epithelia organization, while only 8% (3/37) showed this when the driver was used to express GFP, and 7% (7/99) showed it when using the RNAi lines without the driver (supplementary material Table S1). These results indicate that *sie* is required in the somatic follicle cells for normal epithelial structure or organization. While we did not observe this defect in RNAi knock down experiments using germ line specific drivers, the difficulty of knocking down gene function in older female germ cells prevents us from assessing the germ line requirement for this phenotype using this approach.

Sosie and the actin cytoskeleton

The analysis of *karst* mutants revealed no essential requirement for β_H-Spectrin in organizing or stabilizing the F-actin cytoskeleton (Thomas et al., 1998). To study the role of *sie* in F-actin organization, we analyzed *sie* mutant egg chambers stained for filamentous actin with fluorescently labeled Phalloidin. While apical F-actin accumulation appeared normal in follicle cells (Fig. 5D,E), cortical F-actin structures and plasma membranes of some nurse cells degenerated during mid-oogenesis. This led to the appearance of binucleate nurse cells (Fig. 6A,B). Remnants of degenerating ring canals were also observed between the nuclei of binucleate nurse cells (Fig. 6B). Three pieces of evidence confirm that these phenotypes are due to degeneration of cortical F-actin and cytoplasm membrane structures and not due to defective cytokinesis during cystoblast divisions. First, the total number of intact ring canals and remnants was 15 per egg chamber, indicating that cytokinesis had proceeded normally. Second, defects were not observed before stage 9 and were mostly seen in stage 10 egg chambers. Third, affected ring canals had accumulated Adducin-like Hu-Li Tai Shao protein, a ring canal component that is only loaded onto these structures after cytokinesis (Fig. 6B,C) (Robinson et al., 1994). Like all *sie* phenotypes, the penetrance of these defects varied, ranging from virtually none to up to approximately a quarter of stage 10 egg chambers affected. Despite this variability, the phenotype could clearly be rescued by a sie^+ transgene, proving that sie^+ plays an important role in cortical stability (Fig. 6D).

Reduction of *sie* activity also leads to a less pronounced and more irregular F-actin cortical staining pattern in the germ line.

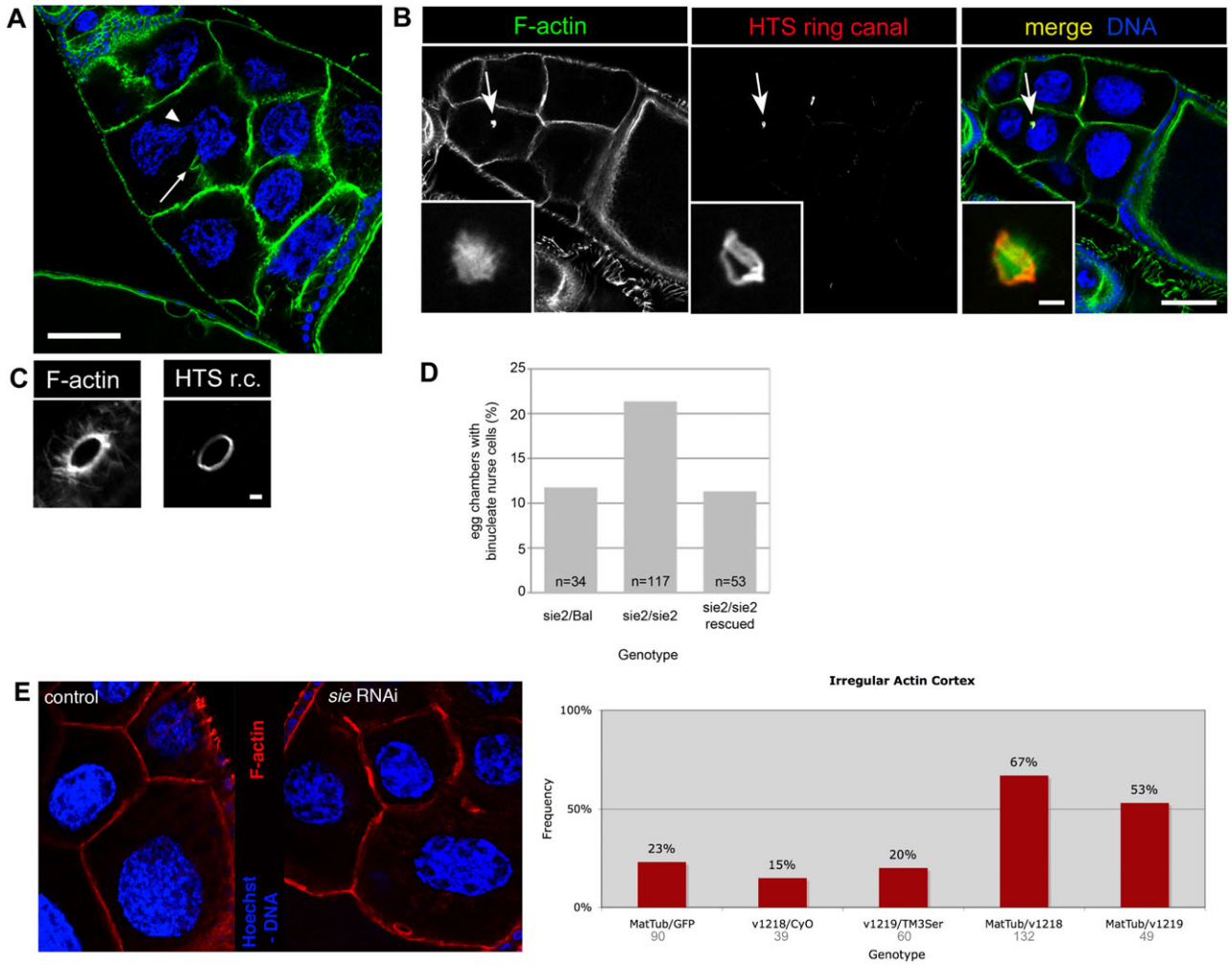

Fig. 6. Loss of *sosie* function leads to degeneration of actin structures in older egg chambers. (**A**) sie^4/sie^4 stage 10 egg chamber. Arrow points to a degenerated F-actin cortex between two nurse cells. In this binucleate nurse cell two nuclei appear to "kiss" one another (arrowhead). Scale bar represents 50 µm. (**B**) Stage 10 sie^2/sie^2 egg chamber with a binucleate nurse cell containing a degenerating ring canal (arrow). Insets show a magnified view of another example of a degenerating ring canal. Note the amorphous F-actin staining and the, although distorted, still ring shaped structure for the inner rim component Adducin-like/Hu-Li Tai Shao r.c. Scale bar represents 50 µm in the main panel and 2.5 µm in the inset. (**C**) Morphology of a wild-type ring canal revealed by staining for F-actin and HTS r.c. Note the very regular ring form and the actin filaments extending from the ring canal ("actin basket") (Nicolas et al., 2009). Scale bar represents 2.5 µm. (**D**) Quantification of the binucleate nurse cell phenotype. n: number of stage 10 egg chambers counted. Full genotypes: *w*; +/SM1; sie^2/TM3 Sb ("sie2/Bal"). *w*; +/SM1; sie^2/sie^2 ("sie2/sie2"). *w*; $att^{58A}[gsie^+\ w^+]$/+; sie^2/sie^2 ("sie2/sie2 rescued"). (**E**) Germ line knock down of *sie* affects cortical F-actin. *matTubGAL4* driving UAS-GFP as "control" and a representative example of the *sie* RNAi constructs that was scored as defective. F-actin is visualized in red and DNA in blue. Additional controls were the two RNAi lines (v1218, v1219) over the balancers (CyO, TM3Ser). MatTub/v1218: *sie* RNAi construct v1218 driven by the matTubGal4 driver (right panel). MatTub/v1219: *sie* RNAi construct v1219 driven by the matTubGal4 driver.

This is also seen upon RNAi induction in the female germ line using the same combination of constructs and drivers as before (Fig. 6E). About 60% (67% for no. 1218, $n=132$; and 53% for no. 1219, $n=49$) of the stage 5–10 egg chambers in which *sie* RNAi was induced in the germ line, showed defective or reduced cortical F-actin staining. In contrast, the various controls showed this phenotype in only 15%, 20% and 23%. This result points to a role of germ line *sie* in the organization or maintenance of cortical F-actin in the germ line.

To address the question of how lack of *sie* may cause defects in cortical F-actin, we tested whether *sie* controls any of the actin organizers known to be involved in the same processes. Filamin organizes filamentous actin and is required for cell shape change and movement (Flanagan et al., 2001). Filamin, encoded by *cheerio* in Drosophila, also plays a role in FC rearrangements during oogenesis and in BC migration (Sokol and Cooley, 2003). Profilin, encoded by *chickadee* (*chic*), assembles actin filaments and is involved in cell migration (Cooley et al., 1992; Verheyen and Cooley, 1994). dPak regulates the integrity and polarity of the actin cytoskeleton in the follicular epithelium (Conder et al., 2007). We tested for genetic interactions between *sie* and these genes. Transheterozygous combinations with *cheerio* and *chic* revealed strong second site non-complementation for the *cheerio* and *chic* phenotypes of irregular organization of cortical F-actin and second site non-complementation or even enhancement of their delayed BC migration phenotype (Fig. 7A,B). In contrast, no such interaction was seen with the *dPak* mutants (data not shown).

The F-actin cytoskeleton of the nurse cells has been implicated in the transport of nurse cell material into the oocyte, contributing to the growth of the oocyte and egg. Accordingly, mutations that disrupt the actin cytoskeleton during these stages cause the formation of smaller embryos and full disruption causes the "dumpless" phenotype. We therefore used the measurements of embryonic size to find out whether the observed F-actin defects may have a functional significance. Indeed, embryos from sie^2/Df mothers are generally slightly shorter than embryos from heterozygous siblings and a small proportion of eggs laid by *sie* females displays a "dumpless" phenotype (Fig. 7C,D). In addition, mutant eggs also have shorter and sometimes broadened dorsal appendages (Fig. 7C,E).

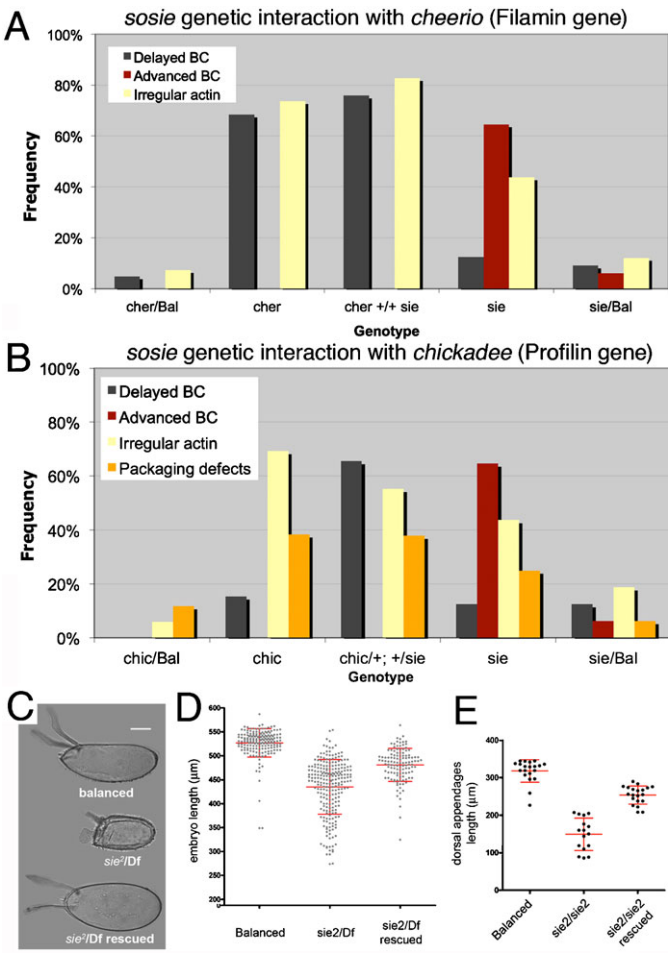

Fig. 7. Interactions between *sie* and actin organizers. (**A**,**B**) *sie* acts as a second site non-complementer for the actin organizers *cher* and *chic*. (A) Enhanced loss of coordination of BC/FC migration and of cortical F-actin integrity in double heterozygous *cheerio* and sie^4 mutants. Egg chambers analyzed are from stage 3 to 10. Number of egg chambers from left to right: $n=41$, 19, 29, 48, 33. (B) Enhancement of the *chic* phenotypes by lack of one copy of *sie*. Cortical F-actin defects, packaging defects and defects in coordination of BC/FC migration are as strong in the double heterozygous *chic*/+; $+/sie^4$ as they are in homozygous *chic* mutants. Egg chambers analyzed ranged from stage 3 to 10. Number of egg chambers inspected: 17, 13, 29, 48 and 16 (from left to right). (**C–E**) Smaller eggs and eggshell defects in *sie* mutants. "Balanced" means sie^2 or Df3R(niki-sie) over a TM3 Sb balancer. "Df" is Df3R(niki-sie). "Rescued" means that in addition to being mutant for *sie*, the female flies had a genomic sie^+ rescue construct (supplementary material Fig. S2A) in the landing platform att^{58A} on the second chromosome. (C,D) Some of the eggs laid by *sie* mutant mothers are short ("dumpless" phenotype) and have rudimentary and broadened dorsal appendages. This phenotype can be rescued by a genomic *sosie* transgene. Note that only a fraction of eggs laid by *sosie* mutant mothers is shorter than normal, and that this fraction has approximately the same size as stage 10 egg chambers that show the F-actin degeneration phenotype (Fig. 6A). Also note that the y-axis starts at 200 µm in D. (C,E) Phenotype (C) and quantitative analysis (E) of the dorsal appendages of eggs laid by sie^2 homozygous mutant mothers. (D,E) each data-point represents one embryo, and bars indicate mean and standard deviations. Scale bar in C represents 100 µm.

Discussion

The Sosie motifs

A motif identified in the predicted extracellular portion of Sosie appears to be an EGF domain. 4 cysteines that maintain the domain structure by forming disulfide bonds (Garrett et al., 2002) are conserved at the same position between human TGF-α, two Drosophila EGF ligands and Drosophila Sosie, and two additional cysteines are present in nearby positions in Sosie (Fig. 3A). It is also noteworthy that two other key residues, a glycine and an arginine close to the C-term of the EGF-like motif (Garrett et al., 2002), are also conserved in Drosophila Sosie. As reviewed by others, EGF domains are widely used protein-protein interaction domains that are frequently found in proteins involved in intercellular signaling or cell adhesion (Hynes and Zhao, 2000; Doroquez and Rebay, 2006). It therefore seems likely that Sosie fulfills a similar cellular function. We also showed that two positively charged residues in positions −3 and −4 from the C-term are essential for Sosie localization to the plasma membrane and hence for the exposure of the EGF-like domain to the extracellular matrix. This suggests that the two residues may be required for proper insertion into the ER membrane and that this is a prerequisite for Sosie to leave the ER and to accumulate preferentially at the plasma membrane. Similarly, it also appears possible that the cytoplasmic domain of Sosie normally serves as an ER export signal as described for

the mammalian type I membrane protein ERGIC-53 with a diphenylalanine (FF) motif in positions −1 and −2 (Kappeler et al., 1997). Although in mammals the F in position −2 is more effective than the F in position −1 (Nufer et al., 2002), it is conceivable that in invertebrates this requirement has evolved differently or that the Sosie sequence is sufficiently effective for the low levels at which Sosie is expressed. Therefore, the mutations we introduced into the Sosie C-terminus may have made this potential ER export signal inaccessible. In support of this hypothesis it is worth mentioning that the ER export of the vertebrate protein ERGIC-53 also requires a minimal tail length and that the export efficiency also depends on an optimal length of the TM domain (Nufer et al., 2003). Changing the dibasic motif in Sosie may have altered the length of the TM and the cytoplasmic domain.

sie and *kst*/β_H-Spectrin act in the same pathway

Different phenotypes associated with *sie* mutations, such as border cells migrating ahead of follicle cells and the distorted appearance of the follicle cell layer that is caused by the bent plasma membranes of the FC, hinted that *sie* may be in the same pathway as *kst* and its protein product β_H-Spectrin. The behavior of different allelic combinations of *sie* and *kst* also points to their involvement in a common pathway. Furthermore, loss of *sie* function leads to loss of apical β_H-Spectrin in some follicle cells of sie^- egg chambers (Fig. 5D,E). This shows that *sie* contributes to localizing or maintaining cortical β_H-Spectrin. However, β_H-Spectrin localization is only affected in some sie^- follicle cells, suggesting that sie^+ acts more to facilitate or support the apical localization of β_H-Spectrin. The apical determinant Crumbs functions in Drosophila to localize β_H-Spectrin apically and to organize the apical spectrin cytoskeleton in some, but not all epithelia (Tepass, 1997; Thomas et al., 1998; Médina et al., 2002). *sie* mutants did not reveal a defect in Crumbs localization, indicating that *sie* does not contribute to β_H-Spectrin localization through Crumbs. Interestingly, loss of Crumbs in follicle cells leads to only a partial reduction of apically localized β_H-Spectrin (Tanentzapf et al., 2000), suggesting the presence of additional mechanism(s) recruiting and/or stabilizing the apical spectrin cytoskeleton in this tissue. The results presented here suggest that Drosophila Sosie could be part of this additional mechanism in the FC epithelium.

How could Sosie function in localizing β_H-Spectrin apically? Sosie::Venus strongly accumulates at apical plasma membranes and is therefore in the right place to participate in organizing the apical spectrin cytoskeleton. However, the cytoplasmic side of Sosie consists of only 5–6 C-terminal amino acids (Fig. 3A). Altering two of these codons prevents the mutant Sosie from reaching the plasma membrane and if this mutant version is expressed in the germ line in a $sie^{-/-}$ background, β_H-Spectrin shows reduced cortical and increased cytoplasmic localization in the germ line, but it does not co-localize with the C-terminally mutated Sie::$Ven^{CtermMut}$ (data not shown). The localization patterns of the mutant Sie::Venus and β_H-Spectrin are consistent with plasma membrane localization of Sosie being required for cortical localization of β_H-Spectrin and with the model that the C-terminal charged residues of Sie contribute to the cortical localization of β_H-Spectrin. Whether these residues are involved in directly binding to spectrin or whether they are only required for membrane localization of Sie, and membrane-bound Sie then binds to spectrin through other factors, still needs to be addressed.

sosie interactions with the actin cytoskeleton

In addition to its role in organizing β_H-Spectrin, *sie* also interacts genetically with the actin organizing genes *cheerio* and *chic* in FC migration (Fig. 7), and its lack causes a variable degree of defects in the organization of the cortical F-actin cytoskeleton. Similar to defects seen in *sie*, mutations in *cheerio* impair proper egg chamber formation by directly preventing extension of centripetal processes and migration of FC around germ line cysts in the germarium (Li et al., 1999; Sokol and Cooley, 1999; Sokol and Cooley, 2003). Our studies now add *sosie* to the small list of genes that seem to have a direct role in the control of FC migration and egg chamber formation. Interestingly, in $cheerio^2$ mutants the plasma membranes between germ cells also frequently dissolve (Robinson et al., 1997; Li et al., 1999). The *cheerio* gene encodes a Filamin, which is related to spectrin with regard to its actin binding domain. Interestingly, filamins have been described to link transmembrane proteins such as integrins to actin (Sharma et al., 1995) and organization of cortical filamentous actin by Filamin is essential to promote cell shape changes and motility (Flanagan et al., 2001). In the Drosophila egg chamber, different mutations in Filamin affect actin filaments in ring canals, at the cortex and also the centripetal cytoplasmic actin filaments (Robinson et al., 1997; Li et al., 1999). While it would be important to study the role of *sie* in Filamin organization, a direct analysis of Filamin distribution is hampered by the fact that the anti-Drosophila Filamin antibody is not available anymore.

Lack of one copy of *sie* makes two actin organizers, *cheerio* and *chic*, haploinsufficient with regard to timely control of BC and FC migration and some *sie* phenotypes also show striking similarities to *chic* mutants (Cooley et al., 1992; Van Vactor et al., 1993; Verheyen and Cooley, 1994; Sokol and Cooley, 2003). *chic* codes for Drosophila Profilin and is required to set up the radial cytoplasmic actin networks correctly. Like *sie* mutants, *chic* mutants also cause the formation of binucleated nurse cells in egg chambers with too few nurse cells. Furthermore, *chic* mutants show defects in extending cellular projections during migration of germarial follicle cells, vitellarial border cells and neuronal growth cones. These interesting parallels make *chic*/Profilin another likely target that could mediate some of the *sie* functions.

Materials and Methods

Drosophila strains

PBac{PB}CG13636^{c03947} and PBac{WH}CG13636^{f00514} are PiggyBac insertions from the Exelixis Collection at Harvard (Boston, MA). Df(3R)Exel6200, *nosGAL4*, *tubGAL4*, eYFP-ER, MB03846, matTubGAL4 (BL no. 7063), UAS-KDEL::RFP, {GawB}109-79, {GawB}109-30, UAS-GFP, $chic^{221}$, $chic^{1320}$, $cher^{2734}$, $cher^{5306}$, $dPak^{6}$, $dPak^{11}$ were obtained from the Bloomington Drosophila Stock Center, and the RNAi lines P{GD250}v1218 and P{GD250}v1219 from the Vienna Drosophila Research Center. kst^1 and kst^2 were from G. Thomas. Re-mobilization of the MB03846 Minos transposon was carried out using a Minos transposase under control of the heat-shock promoter. A 1-hour heat shock in a water bath at 37℃ was applied daily for a total of 5 days during larval development, and transposon excisions were identified by the loss of the GFP marker (present on the Minos transposon) in the progeny of the heat-shocked flies. Screening for imprecise excisions was performed on single fly DNA preparations by polymerase chain reaction using the two forward primers 5′-CACTTGCATTTCGAGCGCGCA-3′ and 5′-GATGACCTCTGGGCATGAG-3′ that bind to the first exons of the predicted *sosie* splice forms RA and RB, respectively, and the reverse primer 5′-CAACATCACTATTGACGGTTG-3′ that binds to the predicted *sosie* neighbor *CG33658*. *Df3R(niki-sie51, 55 and 81)* are

self-made small deficiencies that were created by recombination between the PiggyBac element f00514 and f00361 (Parks et al., 2004; Thibault et al., 2004). They remove *sosie* and 8 genes on its left side (centromeric). Df(*sie*)*22* and *27* were created by recombination between the PiggyBac elements f00514 and e02812. This removed *sosie* and 8 genes to its right (telomeric).

RT-PCR and construction of *sie* transgenes

Total RNA was isolated from dissected ovaries using the RNeasy kit (Qiagen, Hilden, Germany). RT reactions were primed with oligo-dT and performed using a SuperScript reverse transcriptase from Invitrogen (Carlsbad, CA). The subsequent PCRs were done with Taq polymerase (New England BioLabs, Ipswich, MA) and primed with the following oligonucleotides: "a": 5′-CACTTGCATTTCGAGCGCGCA-3′, "b": 5′-CAATTGGGACGTGCGTGGGA-3′, "c": 5′-GAGAGTGCAGTGCCCACGAT-3′, "d": 5′-GGTTAGTGGTAGGGGTAGGATGA-3′. For construction of g*sie*, the genomic region of *sosie*/*CG13636* was PCR amplified from BACR33F18 (BACPAC Resources, Children's Hospital Oakland Research institute) with the primer pair 5′-CGCGTCGACGCACTCCATCCCAGAAGTGG-3′ 5′-CGCGTCGACGATTGCACCAGCAGATCAATGG-3′ using a proofreading Phusion polymerase (Finnzymes, Espoo, FI). Underlined are the SalI restriction sites. After SalI digestion and partial fill-in with dTTP and dCTP, the resulting ~8.4 kilobases product was cloned into the BamHI site of pw+SNattB (Koch et al., 2009; EMBL/GenBank accession no. EU729722), which had been partially filled in with dGTP and dATP. UAS-*sie::Venus* was cloned as follows. First, the *sie* open reading frame coding for the protein isoform PA was PCR amplified from reverse transcribed RNA and cloned into the NotI/XbaI sites of pBS(KS−). Then, site-directed mutagenesis was performed using primer 5′-TGCACGACATCTGCAGTAGATCTAATCTTCAGGGCCTG-3′ and its complementary primer and Phusion polymerase to insert a BglII site (underlined). pCS2-Venus (Nagai et al., 2002) was mutagenized using the primer 5′-CACTCTCGGCATGGACgAGATCTACAAGTAAGAATTCAAGG-3′ and its complementary primer to create the same site (underlined) at the 3′-end of the sequence coding for Venus (*g*: deleted nucleotide). Subsequently, the *Venus* ORF excised with BamHI and BglII was cloned into the BglII site of pBS(KS−)-*sosie*, and clones were screened for orientation by restriction digests. Finally, *sosie*::*Venus* was subcloned into the NotI/XbaI sites of pUASK10attB (Koch et al., 2009; EMBL/GenBank accession no. EU729723). For construction of g*sie::Venus*, an AgeI fragment of g*sie* in pw+SNattB was subcloned into pLitmus28. Then, a BstXI/NarI fragment of pUASK10attB-*sie::Venus*, including the part coding for Venus, was cloned into the BstXI/NarI sites of the pLitmus28 plasmid containing the g*sie* fragment. Finally, the AgeI fragment, now containing the *Venus* coding sequence, was cloned back into the pw+SNattB-g*sie* plasmid. To generate transgenic flies, all constructs were injected into embryos of a *y w*, att2A[*vas*-phi]; attP-58A stock (gift from M. Müller, Basel, Switzerland), where [*vas*-phi] is the bacteriophage φC31 integrase under the control of the *vasa* promoter, and attP-58A the landing platform for insertion of the construct into cytological region 58A (Bischof et al., 2007).

In silico protein analysis

Sosie protein features were predicted computationally with TMHMM for transmembrane domains and SignalP for signal peptides (both from the Center for Biological Sequence Analysis, Technical University of Denmark DTU).

Antibodies, immunostainings and microscopy

Ovary immunostainings were done as previously described (Suter and Steward, 1991). In addition, after the final washes, samples were rinsed 3 times with PBST and washed once with Hoechst and Rhodamine-Phalloidin for 20 minutes in the dark. Finally they were washed twice for 20 minutes each with PBST and then mounted with AquaMount. The following antibodies were used at indicated dilutions: polyclonal anti-Egalitarian at 1:2,000 (Mach and Lehmann, 1997), polyclonal anti-β_H-Spectrin no. 243 at 1:500–1:600 (Thomas and Kiehart, 1994), monoclonal anti-FasciclinIII 7G10 at 1:10 (Patel et al., 1987), anti-Crumbs (1:100), monoclonal anti-Armadillo N2 7A1 at 1:25 (Riggleman et al., 1989), monoclonal anti-Adducin-like/Hu-Li Tai Shao ring canal domain at 1:2 (Robinson et al., 1994), monoclonal anti-Adducin-like 1B1 at 1/40 (Zaccai and Lipshitz, 1996) and anti-Profilin (chi 1J). Monoclonal antibodies were obtained from the Developmental Studies Hybridoma Bank developed under the auspices of the NICHD and maintained by The University of Iowa, Department of Biology, Iowa City, IA 52242. F-actin was stained with Rhodamine-Phalloidin at 1 U/ml, and DNA with Hoechst 33258 at 2.5 µg/ml (both Invitrogen). The following secondary antibodies were also used: Goat anti-mouse Cy3: 1:400 (Jackson Immuno Research), Goat anti-rabbit Cy5 1:80 (Jackson Immuno Research), Goat anti-mouse Cy5: 1:80 (Jackson Immuno Research), Horseradish peroxidase (HRP) conjugated anti-mouse IgG, sheep polyclonal (Amersham Bioscience). For live-imaging of Sosie::Venus, dissected ovaries were separated into single ovarioles and covered with Voltalef oil 3S (VWR, Fontenay, France). Images were recorded either with a Leica TCS-SP2 confocal laser scanning microscope or a Leica DM6000 fluorescence microscope (Leica Microsystems, Mannheim, Germany). In the latter case, deconvolution was subsequently applied using the Leica Application Suite 2.0.2 software. When necessary, contrast enhancements were applied to whole images using Adobe Photoshop.

Acknowledgements

We thank J. Bischof, E. Knust, R. Koch, R. Lehmann, J. Mach, M. Müller and G. Thomas for antibodies, constructs and fly stocks. Special thanks go to M. Müller and M. Affolter for their input, Daniel Hain and Graham Thomas for critical reading of the manuscript, and to Paula Vazquez-Pianzola for valuable advice and help in the lab. We are grateful to R. Stuber Roos, D. Haldemann, A. Walther and T. Rohrer for help with experiments. This work was supported by the Swiss National Science Foundation and the Canton of Bern.

Competing Interests

The authors have no competing interests to declare.

References

Baum, B. and Perrimon, N. (2001). Spatial control of the actin cytoskeleton in Drosophila epithelial cells. *Nat. Cell Biol.* **3**, 883-890.

Bischof, J., Maeda, R. K., Hediger, M., Karch, F. and Basler, K. (2007). An optimized transgenesis system for Drosophila using germ-line-specific phiC31 integrases. *Proc. Natl. Acad. Sci. USA* **104**, 3312-3317.

Bogdanov, M., Xie, J. and Dowhan, W. (2009). Lipid-protein interactions drive membrane protein topogenesis in accordance with the positive inside rule. *J. Biol. Chem.* **284**, 9637-9641.

Brand, A. H. and Perrimon, N. (1993). Targeted gene expression as a means of altering cell fates and generating dominant phenotypes. *Development* **118**, 401-415.

Conder, R., Yu, H., Zahedi, B. and Harden, N. (2007). The serine/threonine kinase dPak is required for polarized assembly of F-actin bundles and apical-basal polarity in the Drosophila follicular epithelium. *Dev. Biol.* **305**, 470-482.

Cooley, L., Verheyen, E. and Ayers, K. (1992). chickadee encodes a profilin required for intercellular cytoplasm transport during Drosophila oogenesis. *Cell* **69**, 173-184.

Dietzl, G., Chen, D., Schnorrer, F., Su, K. C., Barinova, Y., Fellner, M., Gasser, B., Kinsey, K., Oppel, S., Scheiblauer, S. et al. (2007). A genome-wide transgenic RNAi library for conditional gene inactivation in Drosophila. *Nature* **448**, 151-156.

Dobens, L. L. and Raftery, L. A. (2000). Integration of epithelial patterning and morphogenesis in Drosophila ovarian follicle cells. *Dev. Dyn.* **218**, 80-93.

Doroquez, D. B. and Rebay, I. (2006). Signal integration during development: mechanisms of EGFR and Notch pathway function and cross-talk. *Crit. Rev. Biochem. Mol. Biol.* **41**, 339-385.

Flanagan, L. A., Chou, J., Falet, H., Neujahr, R., Hartwig, J. H. and Stossel, T. P. (2001). Filamin A, the Arp2/3 complex, and the morphology and function of cortical actin filaments in human melanoma cells. *J. Cell Biol.* **155**, 511-518.

Garrett, T. P., McKern, N. M., Lou, M., Elleman, T. C., Adams, T. E., Lovrecz, G. O., Zhu, H. J., Walker, F., Frenkel, M. J., Hoyne, P. A. et al. (2002). Crystal structure of a truncated epidermal growth factor receptor extracellular domain bound to transforming growth factor alpha. *Cell* **110**, 763-773.

Goode, S., Wright, D. and Mahowald, A. P. (1992). The neurogenic locus brainiac cooperates with the Drosophila EGF receptor to establish the ovarian follicle and to determine its dorsal-ventral polarity. *Development* **116**, 177-192.

Goode, S., Melnick, M., Chou, T. B. and Perrimon, N. (1996). The neurogenic genes egghead and brainiac define a novel signaling pathway essential for epithelial morphogenesis during Drosophila oogenesis. *Development* **122**, 3863-3879.

Hynes, R. O. and Zhao, Q. (2000). The evolution of cell adhesion. *J. Cell Biol.* **150**, F89-F96.

Kappeler, F., Klopfenstein, D. R., Foguet, M., Paccaud, J. P. and Hauri, H. P. (1997). The recycling of ERGIC-53 in the early secretory pathway. ERGIC-53 carries a cytosolic endoplasmic reticulum-exit determinant interacting with COPII. *J. Biol. Chem.* **272**, 31801-31808.

Khanna, M. R., Stanley, B. A. and Thomas, G. H. (2010). Towards a membrane proteome in Drosophila: a method for the isolation of plasma membrane. *BMC Genomics* **11**, 302.

Koch, R., Ledermann, R., Urwyler, O., Heller, M. and Suter, B. (2009). Systematic functional analysis of Bicaudal-D serine phosphorylation and intragenic suppression of a female sterile allele of BicD. *PLoS ONE* **4**, e4552.

Lee, J. K., Brandin, E., Branton, D. and Goldstein, L. S. (1997). alpha-Spectrin is required for ovarian follicle monolayer integrity in Drosophila melanogaster. *Development* **124**, 353-362.

Lee, S. and Cooley, L. (2007). Jagunal is required for reorganizing the endoplasmic reticulum during Drosophila oogenesis. *J. Cell Biol.* **176**, 941-952.

Li, M. G., Serr, M., Edwards, K., Ludmann, S., Yamamoto, D., Tilney, L. G., Field, C. M. and Hays, T. S. (1999). Filamin is required for ring canal assembly and actin organization during Drosophila oogenesis. *J. Cell Biol.* **146**, 1061-1074.

López-Schier, H. and St Johnston, D. (2001). Delta signaling from the germ line controls the proliferation and differentiation of the somatic follicle cells during Drosophila oogenesis. *Genes Dev.* **15**, 1393-1405.

Mach, J. M. and Lehmann, R. (1997). An Egalitarian-BicaudalD complex is essential for oocyte specification and axis determination in Drosophila. *Genes Dev.* **11**, 423-435.
Margolis, J. and Spradling, A. (1995). Identification and behavior of epithelial stem cells in the Drosophila ovary. *Development* **121**, 3797-3807.
Médina, E., Williams, J., Klipfell, E., Zarnescu, D., Thomas, G. and Le Bivic, A. (2002). Crumbs interacts with moesin and beta(Heavy)-spectrin in the apical membrane skeleton of Drosophila. *J. Cell Biol.* **158**, 941-951.
Metaxakis, A., Oehler, S., Klinakis, A. and Savakis, C. (2005). Minos as a genetic and genomic tool in Drosophila melanogaster. *Genetics* **171**, 571-581.
Mohler, J. and Wieschaus, E. F. (1986). Dominant maternal-effect mutations of Drosophila melanogaster causing the production of double-abdomen embryos. *Genetics* **112**, 803-822.
Montell, D. J. (2008). Morphogenetic cell movements: diversity from modular mechanical properties. *Science* **322**, 1502-1505.
Montell, D. J., Rorth, P. and Spradling, A. C. (1992). slow border cells, a locus required for a developmentally regulated cell migration during oogenesis, encodes Drosophila C/EBP. *Cell* **71**, 51-62.
Nagai, T., Ibata, K., Park, E. S., Kubota, M., Mikoshiba, K. and Miyawaki, A. (2002). A variant of yellow fluorescent protein with fast and efficient maturation for cell-biological applications. *Nat. Biotechnol.* **20**, 87-90.
Ni, J. Q., Zhou, R., Czech, B., Liu, L. P., Holderbaum, L., Yang-Zhou, D., Shim, H. S., Tao, R., Handler, D., Karpowicz, P. et al. (2011). A genome-scale shRNA resource for transgenic RNAi in Drosophila. *Nat. Methods* **8**, 405-407.
Nicolas, E., Chenouard, N., Olivo-Marin, J. C. and Guichet, A. (2009). A dual role for actin and microtubule cytoskeleton in the transport of Golgi units from the nurse cells to the oocyte across ring canals. *Mol. Biol. Cell* **20**, 556-568.
Nufer, O., Guldbrandsen, S., Degen, M., Kappeler, F., Paccaud, J. P., Tani, K. and Hauri, H. P. (2002). Role of cytoplasmic C-terminal amino acids of membrane proteins in ER export. *J. Cell Sci.* **115**, 619-628.
Nufer, O., Kappeler, F., Guldbrandsen, S. and Hauri, H. P. (2003). ER export of ERGIC-53 is controlled by cooperation of targeting determinants in all three of its domains. *J. Cell Sci.* **116**, 4429-4440.
Parks, A. L., Cook, K. R., Belvin, M., Dompe, N. A., Fawcett, R., Huppert, K., Tan, L. R., Winter, C. G., Bogart, K. P., Deal, J. E. et al. (2004). Systematic generation of high-resolution deletion coverage of the Drosophila melanogaster genome. *Nat. Genet.* **36**, 288-292.
Patel, N. H., Snow, P. M. and Goodman, C. S. (1987). Characterization and cloning of fasciclin III: a glycoprotein expressed on a subset of neurons and axon pathways in Drosophila. *Cell* **48**, 975-988.
Peifer, M., Orsulic, S., Sweeton, D. and Wieschaus, E. (1993). A role for the Drosophila segment polarity gene armadillo in cell adhesion and cytoskeletal integrity during oogenesis. *Development* **118**, 1191-1207.
Ran, B., Bopp, R. and Suter, B. (1994). Null alleles reveal novel requirements for Bic-D during Drosophila oogenesis and zygotic development. *Development* **120**, 1233-1242.
Riggleman, B., Wieschaus, E. and Schedl, P. (1989). Molecular analysis of the armadillo locus: uniformly distributed transcripts and a protein with novel internal repeats are associated with a Drosophila segment polarity gene. *Genes Dev.* **3**, 96-113.
Robinson, D. N., Cant, K. and Cooley, L. (1994). Morphogenesis of Drosophila ovarian ring canals. *Development* **120**, 2015-2025.
Robinson, D. N., Smith-Leiker, T. A., Sokol, N. S., Hudson, A. M. and Cooley, L. (1997). Formation of the Drosophila ovarian ring canal inner rim depends on cheerio. *Genetics* **145**, 1063-1072.
Rørth, P. (1998). Gal4 in the Drosophila female germline. *Mech. Dev.* **78**, 113-118.
Ruohola, H., Bremer, K. A., Baker, D., Swedlow, J. R., Jan, L. Y. and Jan, Y. N. (1991). Role of neurogenic genes in establishment of follicle cell fate and oocyte polarity during oogenesis in Drosophila. *Cell* **66**, 433-449.
Sharma, C. P., Ezzell, R. M. and Arnaout, M. A. (1995). Direct interaction of filamin (ABP-280) with the beta 2-integrin subunit CD18. *J. Immunol.* **154**, 3461-3470.
Sokol, N. S. and Cooley, L. (1999). Drosophila filamin encoded by the cheerio locus is a component of ovarian ring canals. *Curr. Biol.* **9**, 1221-1230.
Sokol, N. S. and Cooley, L. (2003). Drosophila filamin is required for follicle cell motility during oogenesis. *Dev. Biol.* **260**, 260-272.
Spradling, A. C. (1993). Developmental genetics of oogenesis. In *The Development Of Drosophila melanogaster* (ed. M. Bate and A. Martinez-Arias), pp. 1-70. Plainview, NY: Cold Spring Harbor Laboratory Press.
Suter, B. and Steward, R. (1991). Requirement for phosphorylation and localization of the Bicaudal-D protein in Drosophila oocyte differentiation. *Cell* **67**, 917-926.
Swan, A. and Suter, B. (1996). Role of Bicaudal-D in patterning the Drosophila egg chamber in mid-oogenesis. *Development* **122**, 3577-3586.
Tanentzapf, G., Smith, C., McGlade, J. and Tepass, U. (2000). Apical, lateral, and basal polarization cues contribute to the development of the follicular epithelium during Drosophila oogenesis. *J. Cell Biol.* **151**, 891-904.
Teasdale, R. D. and Jackson, M. R. (1996). Signal-mediated sorting of membrane proteins between the endoplasmic reticulum and the golgi apparatus. *Annu. Rev. Cell Dev. Biol.* **12**, 27-54.
Tepass, U. (1997). Epithelial differentiation in Drosophila. *Bioessays* **19**, 673-682.
Thibault, S. T., Singer, M. A., Miyazaki, W. Y., Milash, B., Dompe, N. A., Singh, C. M., Buchholz, R., Demsky, M., Fawcett, R., Francis-Lang, H. L. et al. (2004). A complementary transposon tool kit for Drosophila melanogaster using P and piggyBac. *Nat. Genet.* **36**, 283-287.
Thomas, G. H. (2001). Spectrin: the ghost in the machine. *Bioessays* **23**, 152-160.
Thomas, G. H. and Kiehart, D. P. (1994). Beta heavy-spectrin has a restricted tissue and subcellular distribution during Drosophila embryogenesis. *Development* **120**, 2039-2050.
Thomas, G. H., Zarnescu, D. C., Juedes, A. E., Bales, M. A., Londergan, A., Korte, C. C. and Kiehart, D. P. (1998). Drosophila betaHeavy-spectrin is essential for development and contributes to specific cell fates in the eye. *Development* **125**, 2125-2134.
Torres, I. L., López-Schier, H. and St Johnston, D. (2003). A Notch/Delta-dependent relay mechanism establishes anterior-posterior polarity in Drosophila. *Dev. Cell* **5**, 547-558.
Van Vactor, D., Sink, H., Fambrough, D., Tsoo, R. and Goodman, C. S. (1993). Genes that control neuromuscular specificity in Drosophila. *Cell* **73**, 1137-1153.
Verheyen, E. M. and Cooley, L. (1994). Profilin mutations disrupt multiple actin-dependent processes during Drosophila development. *Development* **120**, 717-728.
Zaccai, M. and Lipshitz, H. D. (1996). Differential distributions of two adducin-like protein isoforms in the Drosophila ovary and early embryo. *Zygote* **4**, 159-166.
Zarnescu, D. C. and Thomas, G. H. (1999). Apical spectrin is essential for epithelial morphogenesis but not apicobasal polarity in Drosophila. *J. Cell Biol.* **146**, 1075-1086.